Innovative oxygen carriers uplifting chemical-looping combustion,Chemical-looping combustion, natural gas, integrated project,

(article starts on next page)

GHGT-12

Innovative Oxygen Carriers Uplifting Chemical-looping Combustion

Tobias Mattisson[a]*, Juan Adánez[b] , Karl Mayer[c], Frans Snijkers[d], Gareth Williams[e], Evert Wesker[f], Otmar Bertsch[g], Anders Lyngfelt[a]

[a]*Department of Energy and Environment, Division of Energy Technology, Chalmers University of Technology, S-412 96 Gothenburg, Sweden,* [b]*Instituto de Carboquimica, Miguel Luesma Castan 12, 50015 Zaragoza, Spain,*[c]*Institute of Chemical Engineering, Vienna University of Technology, Getreidemarkt 9/166, A- 1060 Vienna, Austria,* [d]*Flemish Institute for Technological Research (VITO), Unit Sustainable Materials Management, Boeretang 200, B-2400 Mol, Belgium,* [e]*Johnson Matthey, Blount's Court, Sonning Common, Reading RG4 9NH, United Kingdom,* [f]*Shell Global Solutions International B.V., P.O. Box 38000, 1030 BN // Badhuisweg 3, 1031 CM Amsterdam, Netherlands,* [g]*Josef Bertsch Gesellschaft, Herrengasse 23, Postfach 61, 6700 Bludenz, Austria*

Abstract

This paper reports on the main results of the EU-financed project INNOCUOUS (Innovative Oxygen Carriers Uplifting Chemical-Looping Combustion). The project follows a series of successful projects with the aim of developing chemical-looping combustion (CLC) with gaseous fuels rich in methane. The project has included a wide range of experimental and modelling tasks, which included *i)* extensive screening of spray-dried and impregnated oxygen carriers, *ii)* production of impregnated and spray-dried oxygen carriers at >100 kg scale, *iii)* operation of several oxygen carriers at industrial conditions up to 120 kW scale and *iv)* techno-economic study of the next-scale CLC. One area of focus in the project has been the search for viable oxygen carriers which have low or no Ni. A large portfolio of interesting metal oxide systems has been found. Two oxygen carriers of $CaMn_xTi_yMg_{1-x-y}O_3$ were successfully produced in larger amounts by spray-drying and an oxygen carrier of Fe_2O_3/Al_2O_3 was produced in similar quantity using impregnation. The Ca-based material showed excellent behavior in a 10 kW and 120 kW unit, where complete combustion was achieved. With respect to the aim of replacing the bench-mark Ni-based material the project was thus very successful, as complete combustion has never been achieved in these units using Ni-based material.

Keywords: Chemical-looping combustion, natural gas, integrated project, oxygen carrier development

* Corresponding author. Tel.: +46-31-7721425
 E-mail address: tm@chalmers.se

Nomenclature

γ_{CO2} gas yield of carbon in the fuel to CO_2
X_{CH4} methane conversion
η_{FR} combustion efficiency
ϕ oxygen carrier to fuel ratio

1. Introduction

The main difficulty with carbon capture is high energy penalty and costs for gas separation processes, common for pre-combustion capture, post-combustion capture and oxyfuel combustion. The fundamental novelty of chemical looping combustion (CLC) is that no gas separation step is needed at all. Metal oxides are used to transport oxygen from an air reactor to a fuel reactor.[1] The principle ideally allows elimination of the capture penalty. Circulating fluidized bed (CFB) technology is used when constructing a CLC unit, for which there is long commercial experience in power industry with conventional combustion. Moreover, in contrast to pre- and post-combustion capture, chemical-looping combustion readily reaches capture rates of 100%.

In previous EU-projects, chemical-looping combustion for gaseous fuels has developed from a paper concept to actual operation at 120 kW fuel power. Satisfactory fuel conversion performance has been achieved with several nickel-based oxygen carrier materials, e.g. Kolbitsch et al.[2] However, nickel-based materials are expensive and require special environmental/safety precautions. The EU-financed INNOCUOUS project involved a focused search for alternative materials with comparable performance to nickel. This activity is without doubt the most important task to improve the prospects for large-scale deployment of this technology. Two main approaches have been examined:

(i)   nickel-free materials which may or may not take advantage of direct release of gaseous oxygen from the solid (CLOU)

(ii)   the mixed oxides concept, using mainly non-nickel materials with high reactivity towards CO/H_2, together with a minor fraction of particles of reduced nickel content acting as reforming catalyst (i.e. transferring CH_4 to CO/H_2).

The project has utilized a mixture of experimental and theoretical activities, with focus on experimental verification of the process using selected oxygen carrier materials. The project is a joint venture between several academic institutions and industry, with the focus on the following tasks: 1. Development and testing of a large number of spray-dried oxygen carriers which contain no nickel; 2. Development of oxygen carriers by pelletizing and impregnation which contain no or very little Ni;   3. Innovative development of scale up ready particle preparation routes; 4. Testing of new particles under relevant conditions and 5. Overall process integration and CLC next scale design. This paper will report upon the main results of these activities, with focus on oxygen carrier preparation and testing.

2. Oxygen carrier development

In total, more than 150 oxygen carrier materials have been proposed and manufactured by commercially available methods (spray drying or impregnation). Examined materials includes oxides of the transition metals manganese, iron or copper as main active component. In some cases particles were prepared with small amounts of nickel oxide, which could help catalyze homogeneous reactions . Some materials used inert support such as alumina or zirconia to
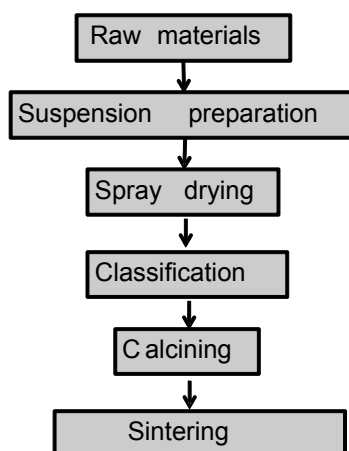
Fig. 1. Process flow diagram of the spray-drying process

achieve sufficient strength and reactivity. Other materials involved several cations present in the form of combined oxides, such as calcium manganite, i.e. $CaMnO_3$. These could have so called uncoupling properties, meaning that they could have a propensity to release oxygen to the gas phase, thus promoting the overall fuel conversion process. [3] Two main manufacturing routes were used: *i)* spray-drying and *ii)* impregnation/pelletizing. Some of the main results for these two classes of materials are given below.

2.1 Spray-dried materials

A total of 60 compositions were spray-dried at VITO, Belgium. Here, oxygen carrier particles with high sphericity, good free-flowing properties and homogeneity on the micro-scale, were prepared by the industrial spray-drying method. The process flow diagram for the production process is shown in Fig. 1. In short, a powder mixture of fine powders of methal oxides were dispersed in de-ionized water with the necessary additives, like binder and dispersant. Appropriate amounts of the above materials were weighed before suspending in de-ionized water. The suspension was homogenized either by milling in a planetary ball mill (Retsch, Germany) for small quantities or by means of an horizontal attrition mill (Netzsch, Germany) for larger amounts.

Spray drying was performed using a Niro 6.3-SD type spray dry plant (Niro, Denmark). The water-based suspension was continuously stirred with a propeller blade mixer while being pumped to the 2-fluid spray dry nozzle. The nozzle is positioned in the lower cone part of the spray drier, so the suspension is sprayed upward. With heated air entering the chamber from the top, a mixed flow pattern is obtained that dries the droplets during the flight. The product is collected at the bottom of the chamber, the material being collected at the cyclone is of too small particle size for the fluidized bed application.

After spray drying, the correct fraction with the required particle size range was separated from the rest of the spray dried product by sieving the chamber fraction. In order to obtain oxygen carrier particles with sufficient mechanical strength, sintering was performed in air at top temperatures in the range of 950°C to 1350°C for 4 hours, using high temperature furnaces (Entech, Sweden; Bouvier, Belgium). Each material was calcined at a minimum of two temperatures, resulting in a total of 130 evaluated oxygen carriers based on spray-drying. After the calcination step, the particles were again sieved to obtain a proper size range, normally in the range 100-200 μm. Table 1 gives an overview of the types of spray-dried oxygen carriers which have been prepared, and also an indication of methane conversion to CO_2, or the gas yield, defined simply as,
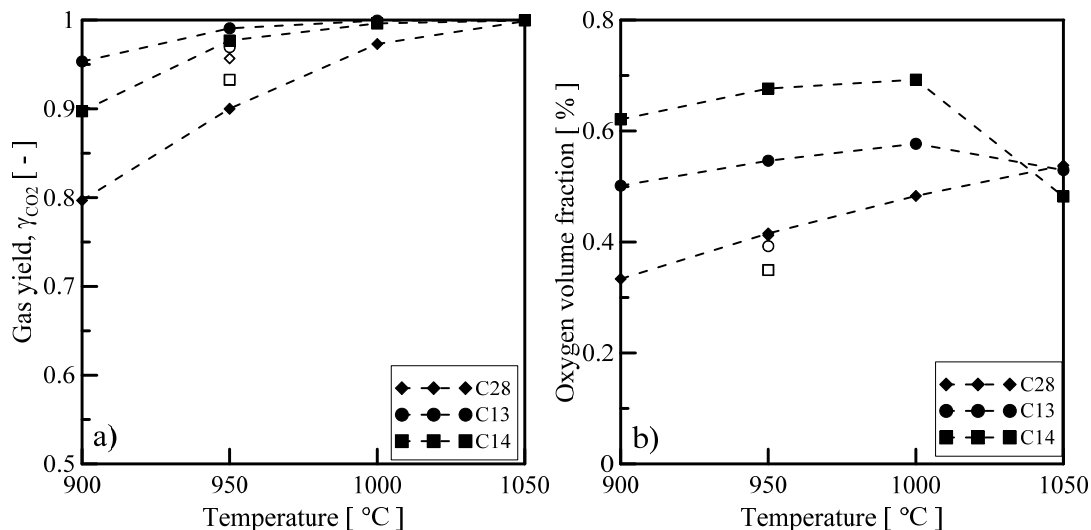
Fig. 2. (a) average γ_{CO_2} and (b) oxygen volume fraction after 360 s inert as a function of temperature for three promising spray dried particles evaluated in a fluidized bed batch reactor. The open symbols refer to a cycle at 950°C conduced after the high temperature test at 1050°C. C13=CaMn$_{0.8}$Mg$_{0.2}$O$_{3-\delta}$, C14=CaMn$_{0.9}$Mg$_{0.1}$O$_{3-\delta}$, C28=CaMn$_{0.775}$Ti$_{0.125}$Mg$_{0.1}$O$_{3-\delta}$. Data taken from Jing et. al., [4, 5]

$$\gamma_{CO_2} = \frac{y_{CO_2}}{y_{CO_2} + y_{CO} + y_{CH_4}} \tag{1}$$

as determined in a batch fluidized bed reactor. As is evident from the table, several oxygen carriers contain more than one active cation, or are so-called combined oxides. These can have several advantages, as earlier outlined by Ryden et al. [6], and generally have oxygen uncoupling properties, meaning that they release oxygen to the gas phase in the fuel reactor. This means that all or part of the fuel actually reacts via normal combustion. Quite clearly, this could have advantages with respect to solid fuels, but perhaps also gaseous fuels. [7] In order to compete with Ni-based oxygen carriers, it was deemed important in the project to produce such materials. As the mechanism for reaction may be different than direct gas-solid reactions, as in CLC, the methane conversion data is simply illustrated as conversion for a certain specific bed inventory of particles, i.e. kg/MW. There is evidently

Table 1. Overview of the type of oxygen carriers evaluated in the project and some indicative numbers of methane conversion as determined in batch tests at 950°C. A reference Ni-material is also included for comparison.

Oxygen carrier	Specific solids inventory	Average gas yield, γ_{CO_2}
1) NiO (VITO-A) (ref)	6 kg/MW	80-90%
2) CaMn$_y$M$_{1-y}$O$_{3-\delta}$	57 kg/MW	86-99%
3) Mn$_{3-y}$Mg$_y$O$_4$	57 kg/MW	46-84%
4) CuO + support material	57 kg/MW	83-100%
5) (Mn$_y$Si$_{1-y}$)O$_x$	57 kg/MW	73-98%
6) Fe$_y$Mn$_{1-y}$)Ti$_x$O$_z$	57 kg/MW	4-76%
7) (Fe$_y$Mn$_{1-y}$)Si$_x$O$_z$	57 kg/MW	45-71%

several systems which have the propensity to convert almost all methane to carbon dioxide at 950°C using only a specific solids inventory of 57 kg/MW of methane. A system of spray-dried oxygen carriers of particular interest was based on the calcium manganite perovskite material $CaMnO_{3-\delta}$. Several materials based on this system were manufactured and the viability of these has been demonstrated by Hallberg et al. [8] Three such oxygen carriers developed in the INNOCUOUS project were $C13=CaMn_{0.8}Mg_{0.2}O_{3-\delta}$, $C14=CaMn_{0.9}Mg_{0.1}O_{3-\delta}$ and $C28= CaMn_{0.775}Ti_{0.125}Mg_{0.1}O_{3-\delta}$. The average reactivity as determined in a batch fluidized bed reactor is shown in Fig 2a, here using a specific inventory corresponding to 57 kg/MW. It can be observed that the yield is very high, above 90% at 950°C and above. However, as is shown in the figure, there is some deactivation of the C13 and C14 after testing at 1050°C, illustrated by the clear loss in reactivity or gas yield. This is not seen for C28, which shows an increased reactivity in the figure. The only difference between C13/C14 and C28 is that the latter includes small amounts of Ti, which likely has a very important effect with respect to stabilizing the perovskite structure. Fig. 2b shows the oxygen volume fraction in the outlet of the batch reactor, when the particles are fluidized with N_2. The particles have CLOU properties, and release oxygen to the gas phase, and the release rate is usually a function of temperature. Also with respect to the uncoupling rate, there is evidence of some type of deactivation for C13/C14, but not for C28.

2.2 Oxygen carriers with low Ni-content

As described in section 2.1, one way to try and approach, or even surpass, the reactivity of Ni-based materials is to use combined oxides with some oxygen uncoupling capabilities. In addition to development of CLOU oxygen carriers, another way of obtaining improved performance of oxygen carriers, is to prepare oxygen carriers using only small fractions of Ni. The idea is that the Ni acts as active sites for reformation of methane to carbon monoxide and hydrogen, but with other metal oxides providing the bulk of the oxygen needed for combustion of the H_2/CO. Here, it may be important to have as high surface area as possible, and thus dry-impregnation was used to manufacture several of the low-Ni systems explored. Three options were explored:

A. The use of a mixture of low cost materials together with an impregnated Ni-based oxygen carrier.
B. Develop oxygen carriers containing in the same particle Fe, Mn or Cu and a small fraction of NiO.
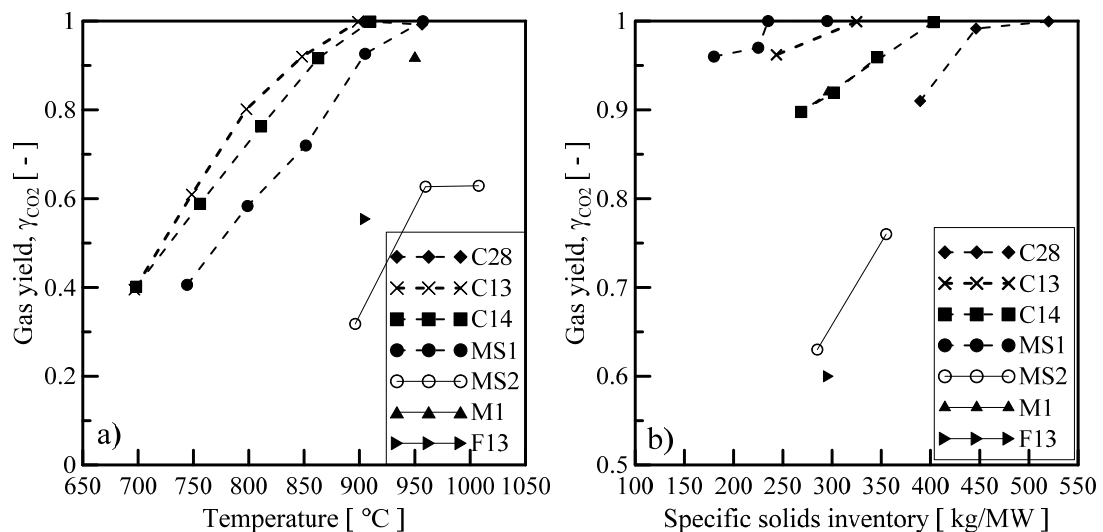C. Improvement of the Ni utilization in highly reactive materials.

Fig. 3. The CO_2 yield as a function of (a) temperature and (b) specific solids inventory for Mn-based combined oxides. In Fig. 3b, temperature is between 900-960°C with the flow to the air reactor $F_{AR, air}$=6 L_N min^{-1}. For nomenclature see Table 4. Part of data is taken from Hallberg et al. [10] The y-scales of the two figures is different.

Table 2. Overview of the oxygen carriers prepared at CSIC by impregnation or pelletization for testing the low-Ni concepts

| Sample	Oxygen carrier	Composition (wt. %)	Sintering T (°C)	Size (µm)	Strength (N)	XRD composition (after calcination)
Ni1 Reference	Ni18-αAl_2O_3	18 % NiO αAl_2O_3	950, 1 h	+100-300	4.1	αAl_2O_3, NiO, $NiAl_2O_4$
FeW1	Fe waste	67.4 % Fe_2O_3 21.3 % Al_2O_3 + others	1200, 6 h	+100-300	2.9	βAl_2O_3, Fe_2O_3, SiO_2
Fe1	Fe15-γAl_2O_3	15 % Fe_2O_3 γAl_2O_3	950, 1 h	+100-300	2.5	αAl_2O_3, Fe_2O_3
Fe2	Fe10-αAl_2O_3	10 % Fe_2O_3 αAl_2O_3	950, 1 h	+100-300	2.8	αAl_2O_3, Fe_2O_3
Fe3	Fe15Ni2- γAl_2O_3	14.3 % Fe_2O_3 2 % NiO γAl_2O_3	950, 1 h	+100-300	1.8	αAl_2O_3, Fe_2O_3, $NiFe_2O_4$
Fe4	Fe14Ni5- γAl_2O_3	13.5 % Fe_2O_3 5 % NiO γAl_2O_3	950, 1 h	+100-300	2.0	αAl_2O_3, Fe_2O_3, $NiAl_2O_4$, $NiFe_2O_4$
Fe5	Fe13Ni12- γAl_2O_3	12.7 % Fe_2O_3 5 % NiO γAl_2O_3	950, 1 h	+100-300	2.7	αAl_2O_3, Fe_2O_3, $NiAl_2O_4$, $NiFe_2O_4$
Mn1	Mn30-γAl_2O_3	30 % Mn_3O_4 γAl_2O_3	950, 1 h	+100-300	2.9	αAl_2O_3, Mn_2O_3, Mn_3O_4
Mn2	Mn17-αAl_2O_3	17 % Mn_3O_4 αAl_2O_3	950, 1 h	+100-300	3.5	αAl_2O_3, Mn_2O_3, Mn_3O_4
Mn3	Mn25Ni2.5- γAl_2O_3	25 % Mn_3O_4 2.5% NiO γAl_2O_3	950, 1 h	+100-300	3.2	αAl_2O_3, $MnAl_2O_4$, $NiAl_2O_4$
Mn4	Mn24Ni9-γAl_2O_3	24 % Mn_3O_4 9 % NiO γAl_2O_3	950, 1 h	+100-300	3.0	αAl_2O_3, $MnAl_2O_4$, $NiAl_2O_4$
Cu1 reference	Cu14- γAl_2O_3	14 % CuO γAl_2O_3	850, 1h	+300-500	2.4	γAl_2O_3, $CuAl_2O_4$, CuO(minor)
Cu2	Cu14Ni3- γAl_2O_3	14 % CuO 3 % NiO γAl_2O_3	850, 1h	+300-500	3.1	γAl_2O_3, $CuAl_2O_4$, CuO, $NiAl_2O_4$ (minor)
NiMgAl1 CLCGASPOWER	Ni20-$MgAl_2O_4$	20 % NiO $MgAl_2O_4$	950, 1h	+100-300	4.3	NiO, $MgAl_2O_4$
NiMgAl2	Ni13- $MgAl_2O_4$	13 % NiO $MgAl_2O_4$	950, 1h	+100-300	2.0	MgO, ZrO_2, NiO(minor), $MgAl_2O_4$, $NiAl_2O_4$
NiCaAl4 CLCGASPOWER	Ni11-$CaAl_2O_4$	11 % NiO $CaAl_2O_4$	950, 1h	+100-300	2.4	NiO, $CaAl_2O_4$, $CaAl_4O_7$
NiCaAl5	Ni10-$CaAl_2O_4$	10.5 % NiO $CaAl_2O_4$	950, 1h	+100-300	1.2	NiO, $CaAl_2O_4$, $CaAl_4O_7$
NiCaAl6	Ni20-$CaAl_2O_4$	20 % NiO $CaAl_2O_4$	950, 1h	+100-300	3.5	$CaAl_2O_4$, $NiAl_2O_4$, NiO (minor)
NiCaAl JM	CLC18NPr(1400) Johnson Matthey	21.5 % NiO	n.a.	+100-200	0.5	NiO, $CaO(Al_2O_3)_2$, $CaO(Al_2O_3)_6$
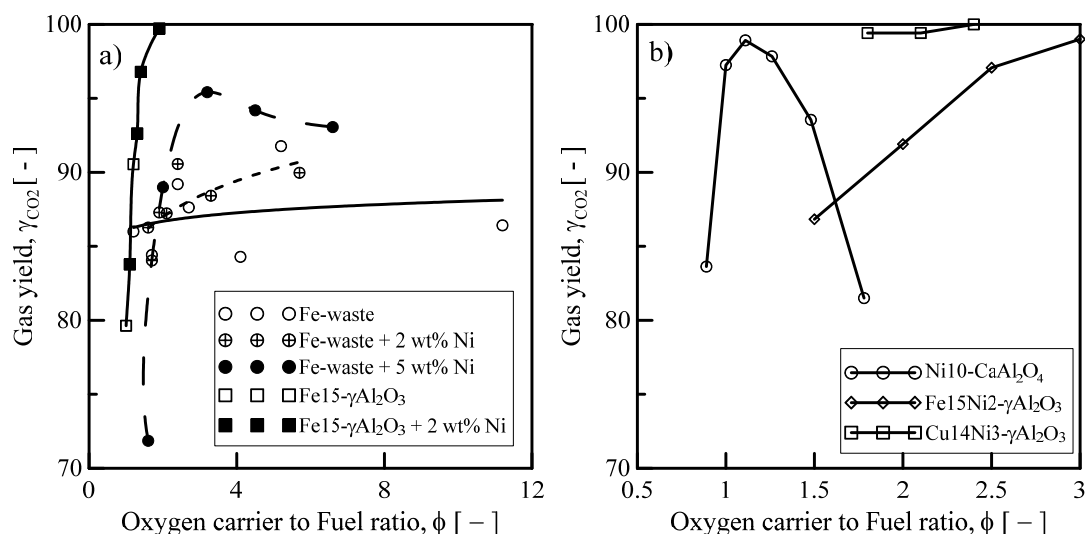
Fig. 4. The CO_2 yield as a function of the oxygen carrier to fuel ratio for (a) iron based materials, alone or mixed with impregnated Ni-materials, (b) three oxygen carriers containing small amounts of Ni. The fuel was methane and the temperature was 900°C for all experiments. Data is taken from [11-15]

Table 3. Overview of selected oxygen carriers tested in the TGA at 950°C. The rate index is calculated using a reference partial pressure of CH_4 of 0.15 atm.

Oxygen carrier	RI (%/min)
Fe waste + Ni18-γAl_2O_3	3.4 / 40
Fe15-γAl_2O_3 + Ni18-γAl_2O_3	7.8 / 40
Fe15-γAl_2O_3	7.8
Fe15Ni2-γAl_2O_3	10.4
Cu15Ni3- γAl_2O_3	19.8*
Ni10-$CaAl_2O_4$	22.0

These options were all explored using either impregnated or pelletized oxygen carriers based on Fe, Cu, Mn and Ni. Table 2 shows the composition of all materials produced. All oxygen carriers were tested using methane in a TGA, and some were rejected based on poor reactivity or mechanical instability. Six materials or combination of materials were selected for testing in a continuous 500 W_{th} CLC unit for CH_4 combustion, see Table 3. Here, the so-called Rate Index (RI) was used to gauge reactivity, a common parameter used for simple and transparent indicator of rates of reaction of oxygen carrier particles. [9]

2.3 Tests of materials in a 300W and 500W continuous CLC reactor

The initial evaluation of the large amount of oxygen carriers was performed using a batch fluidized bed reactor or a TGA. In order to obtain oxygen carrier performance under more realistic conditions, several material or material combinations were evaluated in either a 300W continuous reactor (Chalmers) or 500W reactor (CSIC-ICB) using methane as fuel.

Ten different spray-dried oxygen carrier were identified as promising and have been examined in Chalmers 300 W reactor unit. The materials have been examined both with respect to their capability to oxidize natural gas (CLC), and with respect to their capability to release gas phase oxygen during fluidization with inert gas (CLOU). A list of examined materials can be found in Table 4 with some indication of fuel conversion and attrition also given. As can be seen in Table 4, a majority of the materials showed full fuel conversion also in the 300 W reactor. The performance of all manganese-based materials were quite dependant on temperature and in order to achieve complete conversion, 900°C or above was required, see Fig. 3. In contrast, copper based materials worked well with respect to fuel conversion also at lower temperatures. All materials in Table 4 also released gas phase oxygen at relevant conditions. Unfortunately, several of the examined materials showed quite poor mechanical or chemical stability, i.e. had a rather large or even very large rate of particle attrition during operation. The $CaMnO_3$-based materials performed very well in all aspects. Hence, based on these experiments, C14 and C28 was chosen for up-scaling and further experiments in the 10 kW at Chalmers and 120 kW reactor at TUV.

With respect to the low-Ni materials, these were evaluated in a 500 W reactor at CSIC, also with continuous circulation of particles. The particles shown in Table 3 were used, either as sole oxygen carrier material, or in the case of Fe-based material, also together with some Ni. This was done in order to improve performance. The results are presented in Fig. 4, where the gas yield is shown as a function of oxygen carrier to fuel ratio. In Fig 4a, iron systems are shown, where also experiments were performed with some Ni-material mixed in. The oxygen carrier coming from a waste material, FeW1, needed an addition of 5 wt.% NiO to reach high gas yields, reaching 95% gas yield and full combustion efficiency at oxygen carrier to fuel ratios of 3, with bed inventories of 1900 kg/MW$_{th}$. From Figure 4 it is clear that the impregnated synthetic particle of 15 wt% Fe_2O_3 on γ-Al_2O_3, had complete gas yield at relatively low values of the oxygen carrier to fuel ratio. When the addition of NiO was made to this oxygen

Table 4. Summary of operation in 300 W continuous CLC reactor at Chalmers. All materials were manufactured using spray-drying.

Sample	*Material composition*	*Operational time with fuel [h]*	*Maximum Fuel Conversion [%]*	*Rate of attrition**
C13	$CaMn_{0.8}Mg_{0.2}O_{3-\delta}$	15[1]	100	Low
C14	$CaMn_{0.9}Mg_{0.1}O_{3-\delta}$	16[1]	100	Low
C28	$CaMn_{0.775}Mg_{0.1}Ti_{0.125}O_{3-\delta}$	40	100	Low
M1	$MnMgO_3$	2[2]	93	Moderate
Cu1_950	40 wt% CuO on ZrO_2	2[3]	100	Large
Cu1_1030	40 wt% CuO on ZrO_2	5[3]	100	Large
Cu5	40 wt% CuO on CeO_2	5[3]	100	Large
Cu14	40 wt% CuO on Y-ZrO_2	11[3]	100	Large
MS1	$Fe_{0.66}Mn_{1.33}SiO_3$	7[3]	100	Large
MS2	$FeMnSiO_3$	15[3]	85	Large
F13	$Fe_{0.5}Mn_{0.5}TiO_3$	12	80	Moderate

*Low = less than 0.05wt%/h in filters, moderate = 0.05-0.5 wt%/h, large = more than 0.5 wt%/h.
[1]Experiments aborted due to mechanical failure of reactor.
[2]Experiments aborted due to particle agglomeration.
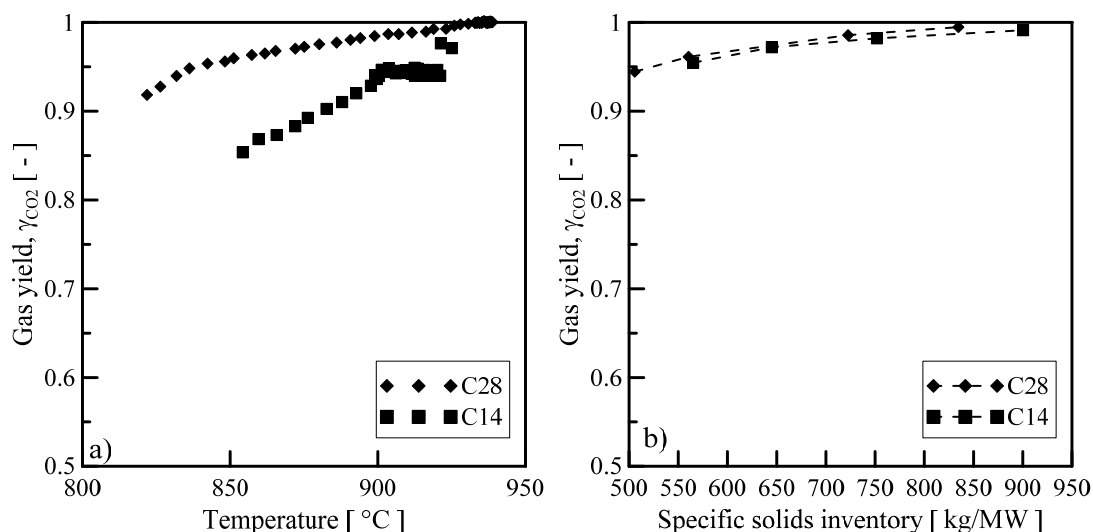*[3]Experiments aborted due to severe attrition and loss of solids circulation.*

Fig. 5. CO_2 yield as a function of a) temperature and b) fuel reactor inventory per fuel power for C14 and C28, tested in the Chalmers 10 kW reactor. The air flow used was $F_{AR, air}$=160 L_N min^{-1} and T_{FR}=930-950˚C in 5b. [10, 16]

carrier, a promoted reactivity effect was only relevant at low temperatures (830°C). At higher temperatures (880°C), the solids inventory necessary to reach full conversion of methane was around 500 kg/MW$_{th}$ which corresponds to a Fe inventory of 50 kg/MW$_{th}$.

The effect of the presence of sulphur in the fuel gas and the attrition behaviour during continuous long term operation was also analysed with the latter impregnated Fe-material. The presence of H_2S in the fuel gas did not affect the combustion efficiency, independently of the amount of S in the gas stream. The results obtained showed that the synthetic Fe-based oxygen carrier developed in this work was not only highly reactive but also sulphur resistant and, consequently, was deemed a suitable material for scale-up. However some improvements in the properties of this material are needed regarding the attrition behaviour and the stabilization of the oxygen transport capacity of the material.

Two combined metal oxides OC materials of Cu-Ni and Fe-Ni were also prepared and tested in the 500 W CLC unit, and the results are displayed in Fig. 4b. No substantial improvement of the combustion efficiency were reached working with the material Fe15Ni2 on γ-Al_2O_3, containing iron and nickel oxides impregnated over the same alumina particle as used for the Fe15 material in Fig 4a. The material, Cu2, Cu14Ni3-γAl_2O_3 was developed previously and contains 3 wt.% of NiO which is present as $NiAl_2O_4$ and improves the attrition resistance at high temperatures. The combustion efficiency of the Cu2 material was investigated using CH_4 containing H_2S. It was found that main part of S was in the FR outlet in the form of SO_2 and only small concentrations (<10 vppm) were present in the AR outlet. At high operating temperatures (850-880°C) combustion efficiency was maintained with time and no loss of carrier reactivity was observed although some S accumulation on the carrier was likely. However, at low temperatures (800 °C) there was a deactivation of the OC and unconverted CH_4 appears in the FR outlet. Therefore, it was concluded that Cu-particles without Ni doping has better possibilities as OC material.

The Ni-based oxygen carrier, Ni10-$CaAl_2O_4$, developed using a resistant support which avoids the NiO-support interaction, was tested in the continuous unit, see Fig. 4b. This material showed very good performance for CH_4 combustion with near complete combustion at oxygen carrier to fuel ratios ranging from 1.0-1.2. A solids inventory in the fuel reactor of 180 kg/MWth was necessary to reach a combustion efficiency of 99 % which corresponds to 15 kg of Ni metal.

3.   Testing at industrial conditions

A total of 16 promising oxygen carrier materials based on widely different compositions and prepared by spray-drying or impregnation were selected and examined in small continuously operating units (300-500 W). From the results of these tests several systems were deemed highly promising, and six materials were judged to fulfil all success criteria set-up for a viable oxygen carrier, and thus selected to be included in a portfolio of oxygen carriers. Two spray-dried oxygen carriers were tested in Chalmers 10 kW unit, where the particles are exposed to velocities similar to those in an industrial boiler. Further, three materials and one material mixture were selected and examined under realistic conditions in the large 120 kW unit in Vienna.

3.1 Tests in Chalmers 10 kW circulating reactor

Based on the experiments in the 300 W reactor the oxygen carrier materials C14 and C28 were produced in new batches of 25 kg each and used to perform additional experiments in Chalmers 10 kW reactor. This reactor involves gas velocities relevant for comparison to large-scale units, i.e. around 3 m/s in the riser, 8 m/s in the cyclone inlet and 20 m/s from air inlet nozzles. Because of this, experiments performed in this reactor should give a much better idea about the performance of oxygen carrier materials during real-world conditions. C14 was operated for 55 h with natural gas combustion and C28 was operated for 100 h, also with natural gas. [10, 16]

Both materials gave very high conversion of the fuel and had low rate of attrition. It was also shown that very low concentrations of methane, carbon monoxide and oxygen at the outlet of the fuel reactor could be obtained simultaneously with both of the materials. Both C14 and C28 were capable of providing full conversion of fuel at certain conditions. Temperature, rate of solids circulation and air ratio was identified as important factors to achieve high fuel conversion. Figure 5a shows an example of the effect of circulation on the gas yield to carbon dioxide. Fig. 5b shows the gas yield as a function of the specific fuel reactor inventory. Both C14 and C28 were found to have very good resistance towards attrition, even though C28 provided quite a lot of fines during the first few hours of operation. From the measured fraction of fines in the elutriated material during the operation in the 10 kW reactor it was concluded that both C14 and C28 can withstand longer continuous operation. An approximate life time of 12 000 h for C14 and an approximate life time of 9 000 h for C28 were estimated.

From the data for the calcium manganite oxygen carriers in the 10 kW, it appears as if full fuel combustion is possible at conditions which approximately correspond to 700-800 kg/MW at normal combustion temperatures. In comparison, a Ni-based oxygen carrier in the same unit, 98% gas yield was found at a specific inventory of 500 kg/MW.[17]

3.2 Tests in Vienna 120 kW circulating reactor

The 120 kW in Vienna has been used in several prior EU-based projects to test viable oxygen carriers, in a similar way as was done in this project. The unit has been described in detail elsewhere. [18] In this project, several oxygen carriers were tested, as can be seen in Table 5. Initial tests were mixed oxide tests, similar to those performed in the 500 W reactor shown in Fig 4a. The aim of this experimental study was to quantify the influence on fuel conversion performance of mixing a highly active Ni-based reforming catalyst in addition to a natural iron-based bulk oxygen carrier, ilmenite, in the 120kW CLC pilot plant. For the experiments, a mixture of the ilmenite and artificial Ni-19γ-Al$_2$O$_3$ particles was chosen as oxygen carriers. The mineral ilmenite, which is mainly FeTiO$_3$, was chosen because of its capability to react with CO and H$_2$ as well as its abundance and low price. Ni-19γ-Al$_2$O$_3$ has been verified in other experiments as a promising reforming catalyst.

From the results of the experimental campaigns with mixed oxides it turned out that the CH$_4$ conversion was not as high as expected, but increased only gradually with catalyst addition from 40% to 50%. This was also observed during the additional experiment with up to 33 kg of Ni-19γ-Al$_2$O$_3$ in the 85 kg mixture. For syngas (1:1 CO:H$_2$) the CO conversion even decreased with addition of catalyst, proving a higher reactivity of ilmenite for CO conversion compared to Ni-19γ-Al$_2$O$_3$. The H$_2$ conversion stayed about constant. Several reasons may contribute to the low conversion efficiency and the low effect of the catalyst in the investigated conditions. The most probable

Table 5. Summary of materials tested in the Vienna 120 kW reactor

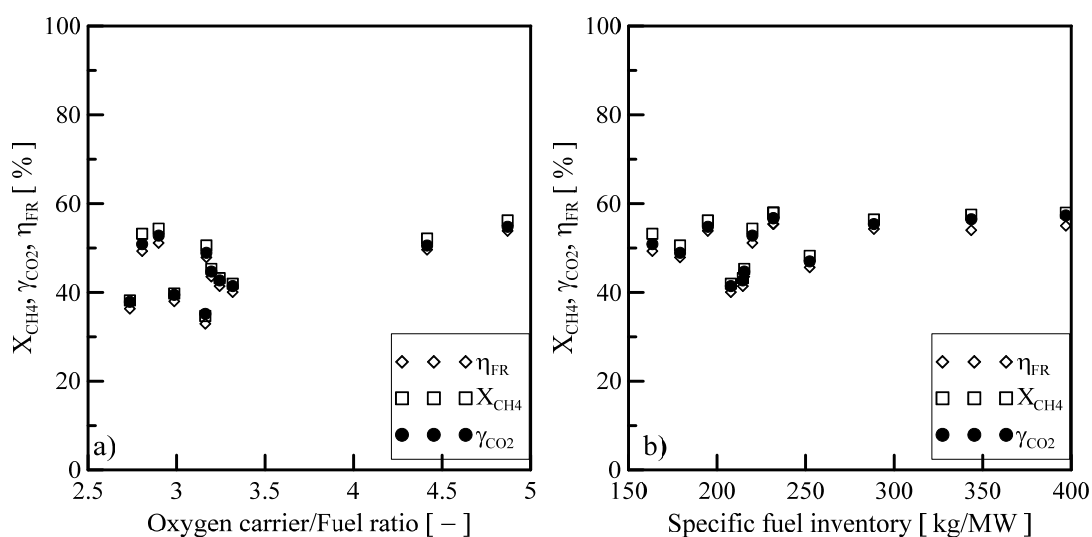| | $m_{solid, act}$ [kg] | λ_{eff} [-] | $P_{fuel\ FR}$ [kW] | ϑ_{FR} [°C] | Operating points | Fuel | | |
						n.g.	Propane	Syngas
Mixed oxides	-	0.5 - 1.2	60 - 130	910 - 970	56	x	-	x
C14	18 - 74	1.2 - 2.0	50 - 120	900 - 960	40	x	x	-
C28	12 - 30	1.1 - 1.9	50 - 100	950 - 960	35	x	x	-
Fe17$_{small}$	19 - 27	1.3 - 3.2	40 - 100	940 - 950	32	x	x	-
Fe17$_{large}$	17 - 58	1.5 - 3.7	40 - 90	890 - 970	20	x	-	x

Fig. 6. Main results of the test runs using the Fe17 material. (a) Effect of the oxygen carrier to fuel ratio on the fuel conversion. T_{FR}=950°C, $P_{th,FR}$= 80 – 90 kW, (b) Effect of the specific fuel reactor inventory. T_{FR}= 950°C, $P_{th,FR}$= 40 – 90 KW. [19]

explanation is that Ni-19γ-Al$_2$O$_3$ as NiAl$_2$O$_4$ (nickel spinel) is so stable even under the conditions in the fuel reactor that no metallic Ni is formed which would be necessary for a fast reforming reaction of CH$_4$. The presence of NiO as Ni-19γ-Al$_2$O$_3$ exhibits slow reduction kinetics compared to the low mean residence time in the reactor. Locally, in the emulsion phase of the fluidized bed, there may be lower CO/CO$_2$ and H$_2$/H$_2$O ratios because of the presence of Fe$_2$O$_3$/Fe$_3$O$_4$ and Fe$_2$TiO$_5$/FeTiO$_3$, leading to a competition for the CO and H$_2$ respectively. The low reforming activity of non-reduced catalyst leads to the observed low conversion of CH$_4$.

In this second experimental study of the project three oxygen carriers developed within the project were tested under relevant conditions in the 120kW CLC unit at TUV. The oxygen carrier materials investigated were: Fe17 (a Fe – based oxygen carrier of 17 wt% Fe$_2$O$_3$ on γ-Al$_2$O$_3$, and made by impregnation), C14 and C28 (both spray dried materials based on CaMnO$_3$ perovskite structure). The iron-based material is based on the impregnated carrier, evaluated in the 500 W continuous unit at CSIC-ICB, see Fig. 4a. The C14 and C28 are the same material as evaluated in the 10 kW, see Fig. 5. For these tests, each material was produced at >100 kg at VITO (spray-dried material) and by Johnson Matthey (impregnated material).

Below follows the main results of the tests with these three materials:
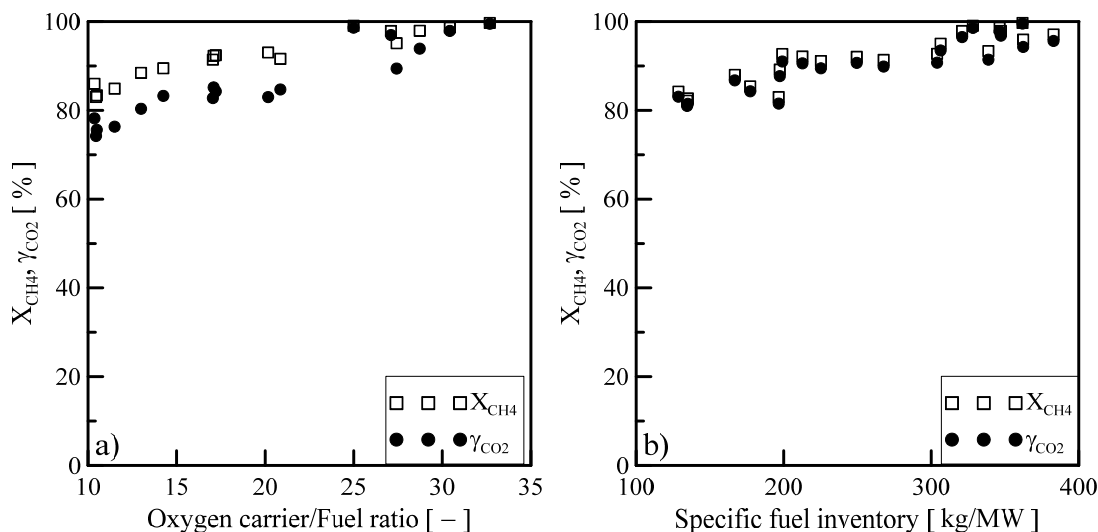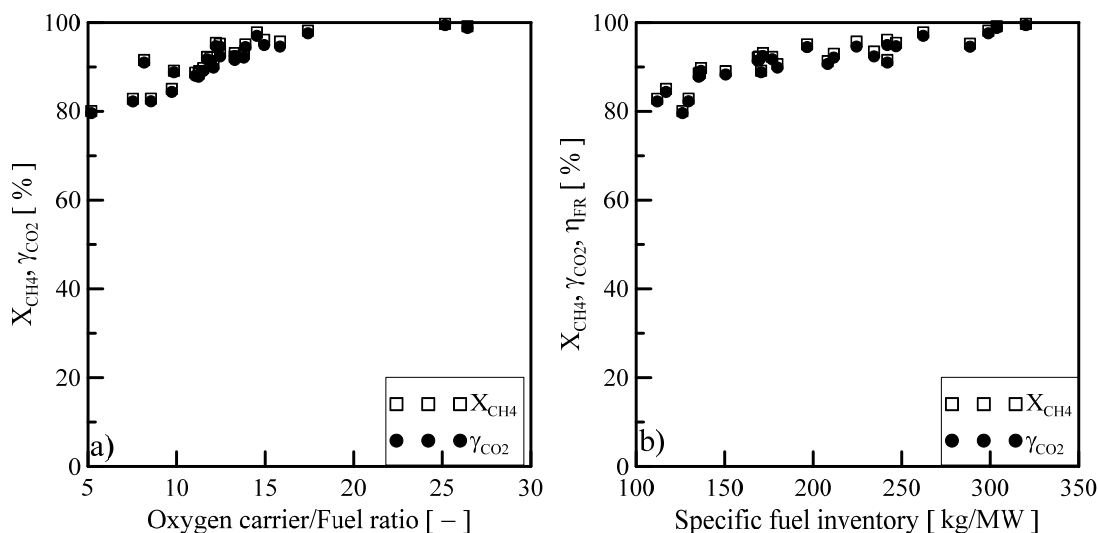
Fig. 7. Main results of the test runs using the C14 material. (a) Effect of the oxygen carrier to fuel ratio on the fuel conversion, (b) Effect of the specific fuel reactor inventory. T_{FR}= 950°C, $P_{th,FR}$= 55 – 120 kW. [19]

Fig. 8. Main results of the test runs using the C28 material. (a) Effect of the oxygen carrier to fuel ratio on the fuel conversion, (b) Effect of the specific fuel reactor inventory. T_{FR}= 950 - 965°C, $P_{th,FR}$= 50 – 85 kW. [19]

Fe17: The methane conversion, combustion efficiency and yield to CO2 can be seen in Fig. 6a. The fuel conversion was lower in the 120kW unit than what was found in the 500 W reactor for a similar material. A fuel conversion of 60% was the best result obtained as shown in Fig. 6. The amount of partially converted fuel (CO and H₂) was low. Increasing fuel conversion could be observed with increasing oxygen availability in the fuel reactor, with increasing oxygen carrier to fuel ratio, see Fig. 6. Increasing the gas solid contact time with higher specific solid inventory in the fuel reactor allows better fuel conversion, as seen in Fig 6b. Analysis of the particles after the experiments showed a significant loss of the active oxygen carrier material, but the loss of iron stabilized after several hours of operation. The particle attrition rate did not decrease, and attrition occurred during the whole period

of oxygen carrier testing.

C14 (CaMn$_{0.9}$Mg$_{0.1}$O$_3$): The C14 oxygen carrier material has been tested in four experiments, which corresponds to about 40 hours of CLC operation. The main results are shown in Fig. 7. With this oxygen carrier stable operation was possible. Experiments showed that higher temperatures give better conversion. During one experiment the air in the air reactor has been diluted with nitrogen to lower the oxygen concentration but the total amount of fluidizing gas was constant to allow comparable solids circulation rates. This investigation showed that lowering the oxygen concentration in the air reactor also lowers the fuel conversion in the fuel reactor. Increasing the solids circulation rate and high oxygen concentrations in the air reactor, which means increasing the oxygen carrier to fuel ratio, allowed full fuel conversion, see Fig. 7. Also a higher specific inventory in the fuel reactor caused better fuel conversion see Fig. 7b. With a specific inventory of about 350 kg/MW in the fuel reactor full fuel conversion was possible. For operating conditions with incomplete fuel conversion also a little amounts of carbon monoxide and hydrogen were present in the fuel reactor off gas. Under operating conditions with full methane conversion no carbon monoxide was present. Oxygen in the fuel reactor off gas was noticeable for operating conditions with good fuel conversion (above 95%) but was at the lower end of the detection limit of the oxygen analyser. Only for operating conditions with full fuel conversion excess oxygen was significantly present in the fuel reactor off gas stream (up to 0.4vol.%wet basis).

In the first period of the testing the attrition rate was quite high, about 1kg/h. After some hours of operation it decreased and stabilized at a moderate value of about 0.6kg/h.

C28 (CaMn$_{0.775}$Mg$_{0.1}$Ti$_{0.125}$O$_3$): Also with this perovskite-type of material full fuel yield to carbon dioxide could be achieved. The temperature dependency was quite similar to the C14 material. High temperatures caused better fuel conversion. The reduction of the oxygen content in the air reactor showed a decrease of the reactivity in the fuel reactor. The material behaved similar to the C14 oxygen carrier. Increasing the solids circulation rate and as a consequence the oxygen carrier to fuel ratio led to full fuel conversion in the fuel reactor as is seen in Fig. 8. Compared to the C14 results almost no partially converted fuel (carbon monoxide and hydrogen) was present in the fuel reactor off gas. Also for operating conditions with low fuel conversion partial fuel conversion did not occur. Oxygen in the fuel reactor off gas was noticeable for operating conditions with good fuel conversion (above 95%) but was at the lower end of the detection limit of the oxygen analyser. A significant increase, like observed with the C14 material, did not occur with the C28 oxygen carrier. The specific inventory to reach full fuel conversion was also in the same range as for the C14. About 320 kg/MW of oxygen carrier in the fuel reactor are necessary to fully convert the fuel in the 120kW
pilot unit.

The C28 showed a high attrition rate at the beginning of the experiments. It was even higher than for the C14. The attrition rate during the first hours of the first experiment was about 1.5kg/h. The attrition rate decreased with time but was higher than for the C14 material. Attrition of the used C28 oxygen carrier was about 1kg/h.

The results shown in Fig 7 and 8 confirms the good results seen in the 10 kW unit for these two materials, and clearly show that the project has been largely successful, and that a viable alternative to NiO has been found. It should be remembered that at no point has full gas fuel conversion and carbon dioxide yield been found in the Vienna unit utilizing Ni-based material.

4. Kinetics and modelling

The kinetics of reactions involved in redox cycles of the C14 and C28 oxygen carriers were determined. Both materials showed oxygen uncoupling, but the oxygen transport capacity for CLOU was relatively low, but could be important under certain conditions, and is likely of significant importance for the high levels of carbon dioxide yield seen in the 10 kW and 120 kW units.

Several redox cycles were performed in a TGA to evaluate possible variations in reactivity and/or oxygen transport capacity of the materials. For C14, the reactivity was not affected signficantly when the solid conversion variations during redox cycles were low; on the contrary, for higher variation of solids conversion the reactivity of the material increased up to the 4th cycle, after which it remained constant. [20] The decrease in the oxygen transport capacity was due to the impossibility to oxidize the material up to the initial oxidation state after a reduction step. Particles that reached the maximum reactivity were denoted as "activated" material. The total oxygen transport capacity for fresh C14 particles was 10%, of which 1.1% corresponded to oxygen uncoupling. After activation, the

total oxygen transport capacity decreased to 7.5%, and the oxygen uncoupling property was near lost. Still, for systems utilizing a high recirculation rate of oxygen carriers, and thus limiting the extent of reduction, an important CLOU property will likely remain.

The grain model was considered for reduction and oxidation reactions and this work is given in detail by de Diego. [20] The particle was assumed to be formed by a certain amount of spherical grains, each following the shrinking core model (SCM) during reduction or oxidation. Some information on the controlling mechanism can be extracted from the shape of the conversion vs. time curves, see Fig. 9. It was observed that reduction with a fuel gas or oxidation by oxygen showed linear dependence on the reacting time at low conversion values, and that the reaction rate decreased over time at higher solids conversion values. In fact, there was a sharp decrease in the reaction rate in some cases. The linear dependence of conversion on time can be attributed to a reaction in the gas-solid interphase with chemical reaction control. It could be speculated that this is due to the oxygen coverage on the surface of the grains being constant during the reduction period. The oxygen diffused from the bulk metal oxide onto the surface where the reaction took place, but this process did not limit the reaction rate under the applied conditions. Additionally, the decrease in the reaction rate at higher conversion values was attributed to a change in the controlling mechanism from chemical reaction to diffusion through the product layer around the grains.

With all the above considerations, and considering the resistance to gas film mass transfer and the diffusion inside the particle to be negligible, the equations that describe this model are the following: [20]

$$t = \tau_{ch} X + \tau_{pl} \left(1 - 3(1 - X)^{2/3} + 2(1 - X) \right))$$ (2)

where X is the degree of solid conversion, t is time and

$$\tau_{ch} = \frac{1}{k_s \left(C_i^n - C_{i,eq}^n \right)}$$ (3)
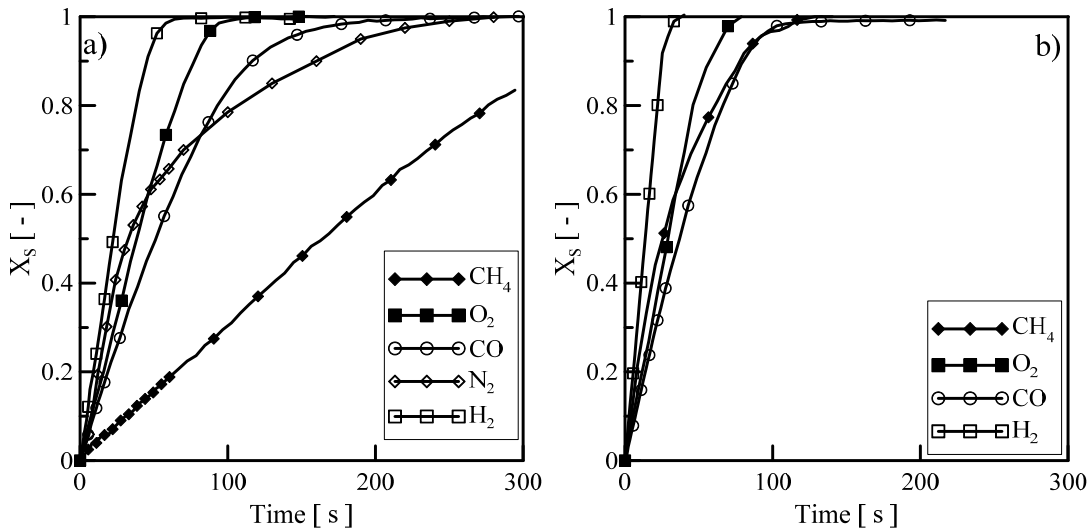
$$k_s = k_{s,0} e^{-E_{ch}/R_g T}$$ (4)

Fig. 9. Conversion vs. time curves during reduction period with CH_4, H_2 or CO and oxidation period by O_2 for (a) fresh particles and (b) activated C14 particles. T = 900°C; fuel: 15 vol.%; O_2: 10 vol.%. Taken from [20].

and

$$\tau_{pl} = \frac{1}{D_{pl} \left(C_i^{n'} - C_{i,eq}^{n'} \right)} \tag{5}$$

where $C_{i,eq}$ is the equilibrium concentration of the reacting gas. The equilibrium concentration of each fuel gas, i.e. CH_4, H_2 or CO, was assumed to be zero; in other words, $CaMn_{0.9}Mg_{0.1}O_{3-\delta}$ was able to fully convert the fuel gas to CO_2 and H_2O.

When a sharp decrease in the reaction rate with time was observed, an additional term that modified the effective diffusivity through the product layer became necessary, with D_{pl} calculated as

$$D_{pl} = D_{pl,0} e^{-E_{pl}/R_g T} e^{-k_X X} \tag{6}$$

where

$$k_X = k_{X,0} e^{-E_X/R_g T} \tag{7}$$

These two equations were only used for reduction of C14 material with CO. In the case of the oxygen uncoupling reaction, the oxygen concentration at equilibrium was considered in the model. Only chemical reaction control was considered, and the evolution of conversion over time was defined by the following equation:

$$t = \frac{1}{k_s \left(C_{O_2,eq}^n - C_{O_2}^n \right)} X \tag{8}$$

Table 6 shows the kinetic parameters determined for C14. The reactivity of C28 also increased with redox cycles. However, this material was more stable than C14 material regarding the oxygen transport capacity. The total oxygen transport capacity only decreased from 8.5% in fresh particles to 8.0% in activated particles. Moreover, the oxygen uncoupling property was maintained during redox cycles, with an oxygen loss of 1.4 wt.% at 1000°C in N_2. This supports the findings of the initial batch experiments, shown in Fig. 2, where a clear deactivation was seen for C14, but not for C28.

Table 6. Kinetic parameters for reaction of fresh C14 particles with CH_4, CO, H_2 and O_2, and oxygen uncoupling in N_2. [20]

			CH_4	H_2	CO	O_2	N_2
n	Order of the reaction	-	0.5	1	1	1	0.5
$k_{s,0}$	Pre-exponential factor of k_s	m^{3n} mol^{-n} s^{-1}	$2.7\cdot10^2$	$7.2\cdot10^1$	$3.1\cdot10^{-1}$	$2.1\cdot10^{-1}$	4.4
E_{ch}	Activation energy for k_s	kJ/mol	107.3	84.7	39.7	25.1	55.6
n'	Order of diffusion	-	0	0	0	1	-
$D_{pl,0}$	Pre-exponential factor of D_{pl}	m^{3m} mol^{-n} s^{-1}	$4.1\cdot10^9$	$6.7\cdot10^8$	$4.9\cdot10^{18}$	$3.1\cdot10^{-2}$	-
E_{pl}	Activation energy for D_{pl}	kJ/mol	291.2	234.2	424.8	13.4	-
$k_{x,0}$	Pre-exponential factor of k_X	-	-	-	$5.4\cdot10^2$	-	-
E_X	Activation energy for k_X	kJ/mol	-	-	43.9	-	-

In this work, an upgrade of an existing mathematical model, developed in the CLC Gas Power project, was also done, both for the fuel and air reactors. [21] Both reactor models were developed in a general form to describe the fluid dynamic of a high-velocity fluidized-bed reactor, and later adapted to the fluid dynamics characteristics of the CLC unit, which is a Dual Circulating Fluidised Bed (DCFB) system. Kinetics for fresh C14 material was used instead of activated C14, as experimental evidence of non-activation was found when very high oxygen carrier circulation rate is used. Fresh C14 material has an important uncoupling activity. Thus, kinetics for oxygen uncoupling reaction was also included in the model.

The linking of the fuel reactor model with the air reactor model allows evaluation of the global performance of the Dual Circulating Fluidised Bed (DCFB) system in the CLC process. Models are solved in an iterative way and the corresponding algorithms in FORTRAN code are developed. A time analogy is used to describe the convergence between both reactors.

The CLC model was validated against experimental results obtained in the CLC unit at Vienna University of Technology (TUV) using the C14 material as oxygen carrier. The kinetic parameters determined in the TGA, see Table 6, was coupled to a hydrodynamic model, and from a mass balance the gas conversion parameters could be obtained. A comparison of the results can be seen in Fig. 10, where the experimental determined values of gas yield, combustion efficiency and methane conversion are compared to the model. In general, good fitting between theoretical and experimental results is obtained, as is shown in Fig. 10. Methane conversion was clearly a function of the operational conditions during the experimental campaign, and these variations were evaluated by a detailed analysis of the theoretical results. At all conditions, the oxygen carrier was highly oxidized in the air reactor. So, oxygen carrier oxidation in the air reactor was not limiting the oxygen availability in the fuel reactor. Incomplete methane conversion was due to the low reactivity of C14 material with methane. However, near complete combustion was reached in some cases, as is evident from Fig 10. Model results confirm this behaviour, and in these cases the relevance of oxygen transference via oxygen uncoupling mechanism became dominant over gas-solid reaction for methane conversion. An increase in the oxygen carrier to fuel ratio and the solids circulation flow rate values favour the oxygen transference by oxygen uncoupling mechanism, and hence the methane conversion is increased.

5. Development of the next-scale CLC boiler

Another part of the project has concerned the development of a process model for chemical-looping combustion. An overall process integration and design for a 10 MW chemical-looping boiler fired by natural gas has been proposed, see Fig. 11. The chemical-looping boiler was applied for steam production for electricity production or industrial use. It was concluded that due to the need of two reactors, the divided flue gas streams and the oxygen
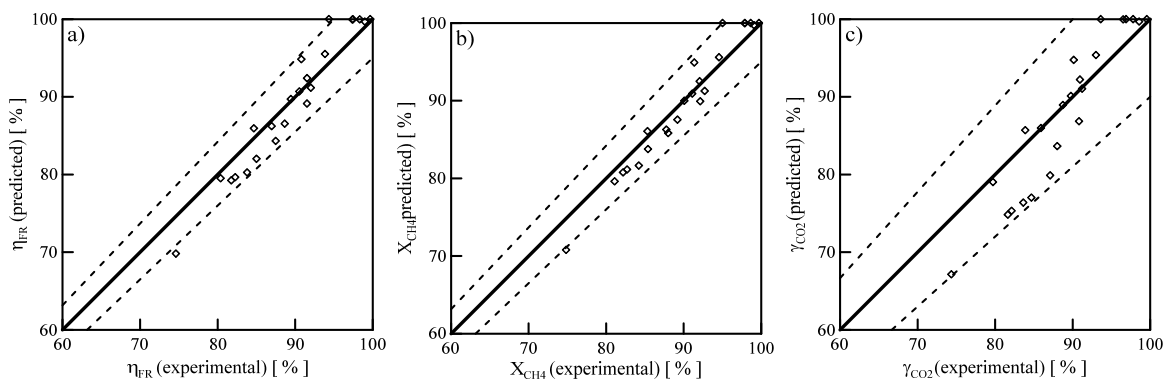

Fig. 10. Comparison between experimental and predicted values of: (a) combustion efficiency, (b) methane conversion and c) gas yield for operation with C14 in the 120 kW CLC unit in Vienna. Dashed lines: deviation boundary of ±5% or ±10% (gas yield). [21]
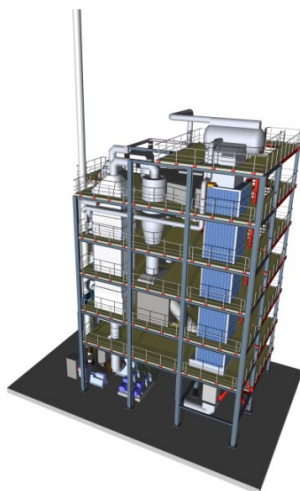
Fig. 11. Layout of next scale 10MW CLC boiler.

carrier system a chemical looping boiler would be more expensive than a common gas-fired boiler. However, the process as a whole looks feasible and attractive since complete carbon dioxide sequestration would be achieved at reasonable cost.

6. Conclusions

Chemical-looping combustion has been pointed out by many researchers as the most viable alternative for carbon capture from natural gas, but has had the drawback that Ni has been the only proven alternative as oxygen carrier. The INNOCUOUS project has taken the technology to the next level of development, with establishment of new and novel oxygen carriers which have proven potential at realistic conditions. Full methane gas yield to carbon dioxide has been possible in both the 10 kW and 120 kW scale using two calcium manganite oxygen carriers. In the larger of the units, full gas yield was achieved using specific inventories of 300-400 kg/MW material, something which has not been achieved using Ni-based material. The high conversion levels is very likely due to some oxygen uncoupling behavior of the used material. As a result of the project a number of other oxygen carrier materials were developed, which also have good potential to be used with gaseous fuel. The production of oxygen carriers at >100 kg has also provided a learning experience on production at larger scale than is normally done within current CLC research, but highly important for the next scale CLC.

7. Acknowlededement

References

[1] M. Ishida, H. Jin, A new advanced power-generation system using chemical-looping combustion, Energy - the International Journal, 19 (1994) 415-422.
[2] P. Kolbitsch, J. Bolhar-Nordenkampf, T. Pröll, H. Hofbauer, Comparison of two Ni-based oxygen carriers for chemical looping combustion of natural gas in 140 kW continuous looping operation, Ind. Eng. Chem. Res, 48 (2009) 5542-5547.

[3] T. Mattisson, A. Lyngfelt, H. Leion, Chemical-looping oxygen uncoupling for combustion of solid fuels International Journal of Greenhouse Gas Control, 3 (2009) 11-19.

[4] D. Jing, T. Mattisson, H. Leion, M. Rydén, A. Lyngfelt, Examination of Perovskite Structure CaMnO3-δ with MgO Addition as Oxygen Carrier for Chemical Looping with Oxygen Uncoupling Using Methane and Syngas, International Journal of Chemical Engineering, (2013) Article ID 679560.

[5] D. Jing, T. Mattisson, M. Ryden, P. Hallberg, A. Hedayati, J. Van Noyen, F. Snijkers, A. Lyngfelt, Innovative Oxygen Carrier Materials for Chemical-Looping Combustion, Energy Procedia, 37 (2013) 645-653.

[6] M. Rydén, H. Leion, T. Mattisson, A. Lyngfelt, Combined oxides as oxygen-carrier material for chemical-looping with oxygen uncoupling Applied Energy, 113 (2013) 1924-1932.

[7] T. Mattisson, Materials for Chemical-Looping with Oxygen Uncoupling, ISRN Chemical Engineering, 2013 (2013).

[8] P. Hallberg, D. Jing, M. Rydén, T. Mattisson, A. Lyngfelt, Chemical looping combustion and chemical looping with oxygen uncoupling experiments in a batch reactor using spray-dried CaMn1- xM xO3-δ (M = Ti, Fe, Mg) particles as oxygen carriers Energy and Fuels 27 (2013) 1473-1481.

[9] M. Johansson, T. Mattisson, A. Lyngfelt, Comparison of oxygen carriers for chemical-looping combustion, Thermal Science, 10 (2006) 93-107.

[10] P. Hallberg, M. Källen, T. Mattisson, M. Ryden, A. Lyngfelt, Overview of operational experiences with calcium manganate oxygen carriers in chemical-looping combustion, in: 3rd Int. Conf. on Chemical looping, Gothenburg, Sweden, 2014.

[11] P. Gayán, A. Cabello, F. García-Labiano, A. Abad, L. de Diego, J. Adánez, Performance of a low Ni content oxygen carrier for fuel gas combustion in a continuous CLC unit using a CaO/Al2O3 system as support, International Journal of Greenhouse Gas Control, 14 (2013) 209–219.

[12] P. Gayan, L. De Diego, F. Garcia-Labiano, J. Adanez, A. Abad, C. Dueso, Effect of support on reactivity and selectivity of Ni-based oxygen carriers for Chemical-Looping Combustion, Fuel, (2008) 2641-2650.

[13] P. Gayán, M. Pans, M. Ortiz, A. Abad, L. De Diego, F. García-Labiano, J. Adánez, Testing of a highly reactive impregnated Fe 2O 3/Al 2O 3 oxygen carrier for a SR-CLC system in a continuous CLC unit Fuel Processing Technology, 96 (2012) 37-47.

[14] M. Ortiz, P. Gayán, L. de Diego, F. García-Labiano, A. Abad, M. Pans, J. Adánez, Hydrogen production with CO2 capture by coupling steam reforming of methane and chemical-looping combustion: Use of an iron-based waste product as oxygen carrier burning a PSA tail gas, J. of Power Sources, 196 (2011) 4370–4381.

[15] M. Pans, P. Gayán, A. Abad, F. García-Labiano, L. de Diego, J. Adánez, Use of chemically and physically mixed iron and nickel oxides as oxygen carriers for gas combustion in a CLC process, Fuel Processing Technology, 115 (2013) 152–163.

[16] M. Källén, M. Rydén, C. Dueso, T. Mattisson, A. Lyngfelt, CaMn0.9Mg0.1O3-δ as Oxygen Carrier in a Gas-Fired 10 kWth Chemical-Looping Combustion Unit, Industrial & Engineering Chemistry Research, 52 (2013) 6923-6932.

[17] T. Mattisson, E. Jerndal, C. Linderholm, A. Lyngfelt, Reactivity of a spray-dried NiO/NiAl2O4 oxygen carrier for chemical-looping combustion, Chem. Eng. Sci., 66 (2011) 4636-4644.

[18] K. P, P. T, B.-N. J, H. H, Design of a Chemical Looping Combustor using a Dual Circulating Fluidized Bed (DCFB) Reactor System, Chem Eng Technol 32 (2009) 398-403.

[19] K. Mayer, S. Penthor, T. Pröll, H. Hofbauer, The different demands of oxygen carriers on the reactor system of a CLC plant – results of oxygen carrier testing in a 120kW pilot plant, in: The 3rd International Conference on Chemical looping, Gothenburg, Sweden, 2014.

[20] L. de Diego, A. Abad, A. Cabello, P. Gayan, F. García-Labiano, J. Adánez, , Reduction and oxidation kinetics of a CaMn0.9Mg 0.1O3-δ oxygen carrier for chemical-looping combustion Industrial and Engineering Chemistry Research, 53 (2014) 87-103.

[21] A. Abad, P. Gayán, L. de Diego, F. García-Labiano, J. Adánez, K. Mayer, S. Penthor, Modelling a CLC process improved by CLOU and validation in a 120 kW unit, in: F.W. Jinghai Li, Xiaojun Bao and Wei Wang (Ed.) 11th International Conference on Fluidized Bed Technology, Beijing, China, 2014.